

## Satellite Recording and Modeling of Short Internal Waves in Coastal Zones of the Ocean<sup>1</sup>

Academician of the RAS V. G. Bondur<sup>a</sup>, Yu. V. Grebenyuk<sup>a</sup>, and E. G. Morozov<sup>b</sup>

Received July 16, 2007

DOI: 10.1134/S1028334X0801042X

Analysis of generation conditions of short internal waves in the coastal zones of the ocean based on the spectra of satellite images obtained with high-resolution optical equipment and mathematical modeling showed that such high-frequency internal waves can develop during the formation of a sharp thermocline (pycnocline) near the surface. They can exist only in a thin pycnocline and do not penetrate to the depths of the ocean.

### PECULIARITIES OF THE STUDY BASIN

The investigations were carried out south of Oahu Island (Hawaii). Study of tidal internal waves in the region (the results are described in [1, 2]) revealed that the main generation of internal tide occurs at depths greater than 700 m. Figure 1 presents a fragment of the chart of the study region south of Oahu Island with bottom topography. Figure 2 shows the profile corresponding to the AB direction. This profile evidences sharp slopes of the bottom at distances of ~3 km and ~40 km off the coast.

Tidal internal waves generated in the deep part of the Hawaiian Ridge propagate to the ocean off the coast, while their second component is directed to the coast [1, 2]. This component and horizontal currents generated by this component can serve as the generator of secondary internal waves at the slope of the shelf at depths slightly greater than 50 m (Fig. 2).

Internal waves in the ocean are usually long waves. This is evidenced by observations from space [3–5].

Their depth is at least greater than the depth of the ocean [6]. This can be demonstrated on the basis of the dispersion relation. The characteristic value of the

Brunt–Väisälä frequency  $N = \sqrt{\frac{g}{\rho_0} \frac{d\rho_0}{dz}}$  in the upper layer of the ocean in this region is approximately equal to  $\sim 0.01 \text{ s}^{-1}$  [7]. The corresponding limiting periods of short-period internal waves are equal to a few minutes. Then, the dispersion relation for internal waves [8]

$$L = \frac{NHT}{\pi n}, \quad (1)$$

where  $n$  is the mode number ( $n$  is equal to 1 or 2),  $L$  is the wavelength,  $T$  is period,  $H$  is depth of the sea, shows that even 5-min waves should be approximately 0.5 km long at a depth of ~400 m (for  $n = 1$ ). More accurate solutions based on the real vertical distribution of the Brunt–Väisälä frequency do not lead to a significant decrease in the wavelength for short-period waves.

Thus, short internal waves with lengths ~100 m should not exist at mean ocean stratification in this region. However, such waves can be recorded from space, as will be shown below.

### RESULTS OF SHORT-PERIOD INTERNAL WAVE RECORDING BASED ON THE SPECTRA OF SATELLITE IMAGES

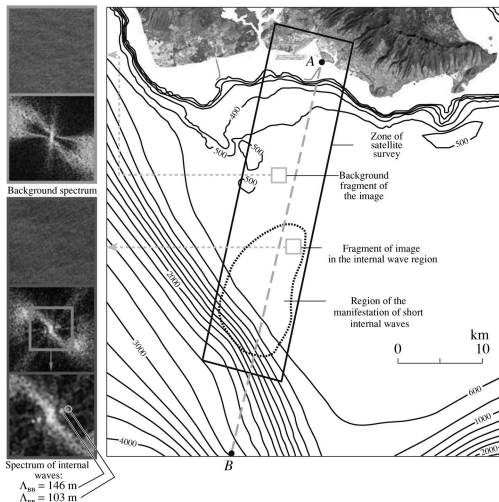
In 2002–2004, a survey of Mamala Bay of Oahu Island (Hawaii) was carried out using high-resolution (0.6–1.0 m) optical equipment installed on the QuickBird and IKONOS satellites [3, 9–13]. Figure 1 shows an example of the survey zone in the study region from the IKONOS satellite on September 2, 2002 [3, 9]. Surface manifestations of internal waves were recorded by means of spatial spectral processing of fragments of satellite images [13].

Figure 1 presents the results of spectral processing of two fragments of a satellite image obtained on September 2, 2002. Spatial frequency spectra of one of the fragments of the image with a size of  $2 \times 2 \text{ km}$

<sup>1</sup> This article was translated by the authors.

<sup>a</sup> Aerocosmos Scientific Center for Aerospace Monitoring, Gorokhovskii pr. 4, Moscow, 105064 Russia

<sup>b</sup> Shirshov Institute of Oceanology, Russian Academy of Sciences, Nakhimovskii pr. 36, Moscow, 117997 Russia; e-mail: egmorozov@mail.ru



**Fig. 1.** Fragment of the chart of the study region near Oahu Island (Hawaii) and results of spectral processing of the fragments of satellite image obtained on September 2, 2002 from the IKONOS satellite (resolution is 1 m).

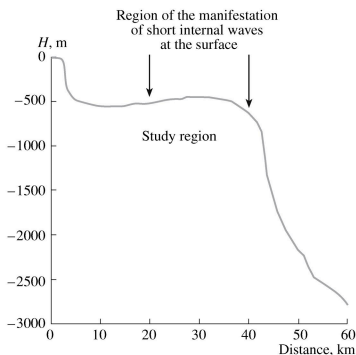


**Fig. 2.** Profile of the bottom along profile AB (see Fig. 1) in the study region.

(2048 × 2048 pixels) at a distance of ~22.5 km from the coast are shown below on the left side in this figure. The lower spectrum is shown with magnification for better visualization. Two pairs of local spectral harmonics caused by high-frequency internal waves are clearly seen in these spectra. The wavelengths corresponding to these spectral harmonics are equal to 103 and 146 m. Such maxima are not distinguished (Fig. 1, upper left side) in the spectrum of a similar fragment recorded closer to the coast (at a distance of ~17 km).

Parameters of short-period internal waves, their lengths, and directions of propagation were calculated from the results of spectral processing of fragments of a number of space images obtained in August–September of 2002–2004 from the IKONOS and QuickBird satellites. The wavelengths varied within 80–200 m, and their propagation directions changed within ~30°–60°, which is close to the orthogonal direction with respect to the isobaths [13]. The manifestation region of such short internal waves distinguished from the spectral maxima of satellite images is bounded by a dashed line in Fig. 1 and indicated with arrows in Fig. 2. Thus, processing of the data allowed us to reveal local maxima in the spectra of satellite images of the ocean sur-

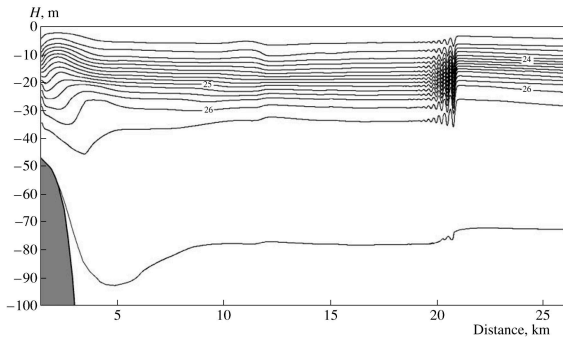


Fig. 3. Packet of short internal waves and field of specific densities over AB section (see Fig. 2) directed to the open ocean after calculations during four tidal periods M2 from the beginning of calculations.

face caused by short-period internal waves (with lengths  $L \sim 100$  m), which are prominent at distances of 20–40 km off the coast [13]. Owing to the masking influence of the surface wind waves, these short internal waves are not found visually in the initial satellite images as usually happens in many regions in the case of longer wavelengths [3–5]. Therefore, short internal waves can be selected only based on the results of spectral analysis of the images [3, 9].

Let us consider conditions under which the existence of short internal waves and their manifestation at the ocean surface are possible. Packets of short-period internal waves are generated when internal tidal waves break. The frequency of such waves is close to the Brunt–Väisälä frequency. If a sharp thermocline is formed at small depths in specific conditions, e.g., when the surface warms up (this usually occurs in August–September in the study region) [7, 11, 12], higher frequency waves can form at the thermocline. These waves cannot propagate deeper than the thermocline due to their specific properties. The Brunt–Väisälä frequency deeper than the upper pycnocline (thermocline) should be lower than the frequency of the high-frequency waves. This condition forbids physically their propagation to the depths. The depth of the ocean is not important for such waves. The pycnocline thickness will be the characteristic depth scale for such waves. Such short waves can exist at the pycnocline and manifest themselves at the surface if this pycnocline is not deep, for example its depth and thickness are equal to ~10–15 m. Let us analyze this situation from the theoretical point of view.

#### THEORETICAL PREREQUISITES FOR THE POSSIBILITY OF GENERATION OF ULTRASHORT INTERNAL WAVES

Let us consider linearized hydrodynamic equations with respect to the unperturbed state specified by the hydrostatic equation. All unknown variables except for the vertical velocity component were excluded from the equations [8]. In the Boussinesq approximations, when we neglect density variations  $\rho_0(z)$  along horizontal axes, the equation for the vertical velocity component is written as

$$\Delta w_{tt} + N^2 \Delta_2 w + f^2 w_{xx} = 0, \quad (2)$$

where  $w$  is the vertical velocity component,  $t$  is time,  $f$  is the Coriolis parameter, and  $\Delta_2$  is 2D Laplacian in horizontal coordinates.

Let us formulate the boundary conditions. At the bottom, at  $z = -H = \text{const}$ , the vertical velocities are equal to zero:

$$w(-H) = 0. \quad (3)$$

At the surface, we can also assume that velocity is zero, but due to the considerations of surface motions caused by internal waves, we shall consider that pressure variations at the surface are equal to zero; i.e.,

$$\frac{dP}{dt} = 0 \text{ at } z = \zeta(x, y), \quad (4)$$

where  $\zeta(x, y)$  are deviations of the free surface from the unperturbed state at  $z = 0$ .

In this relation, pressure  $P$  is the sum of the constant component of pressure  $p_0$  and fluctuations  $p$ :  $P = p_0 + p$ .

Let us linearize the condition of constant pressure at the free surface with account for the hydrostatic equation and exclude pressure from it using the equations of motion. As a result, we obtain the following relation:

$$(w_{,zz} + f^2 w)_{,z} - g \Delta_z w = 0 \text{ at } z = \zeta \approx 0. \quad (5)$$

The solutions in the form of plane waves always exist for Eq. (2)

$$w = \varphi(z) e^{i(k_x x + k_y y - \omega t)}, \quad (6)$$

where  $\varphi(z)$  is the amplitude function.

Substituting Eq. (6) and boundary conditions (3) and (5) into Eq. (2), we get

$$\frac{d^2 \varphi}{dz^2} + \frac{N^2(z) - \omega^2}{\omega^2 - f^2} k^2 \varphi = 0, \quad (7)$$

$$\frac{\omega^2 - f^2}{k^2 g} \frac{d\varphi}{dz} - \varphi = 0; \quad \varphi(-H) = 0 \text{ при } z = 0. \quad (8)$$

In these equations  $k^2 = k_x^2 + k_y^2$ .

Let us simplify the boundary condition at the free surface assuming  $\varphi(0) = 0$ . Thus, we filter out surface waves.

It is clear that Eq. (8) in the oceanic conditions can be solved if condition  $N > \omega > f$  is satisfied. If the wave frequency in the near-surface pycnocline is high and exceeds the Brunt–Väisälä frequency ( $\omega > N$ ) in the layer under this thin pycnocline, the waves would propagate in the density jump layer without spreading deeper in the ocean.

The simplest form of solution for the amplitude function at a constant value of the Brunt–Väisälä frequency is a sinusoidal function of depth with zero values at the surface and bottom. Then, instead of amplitude function  $\varphi(z)$ , it is possible to use vertical velocity  $w$  or the amplitude of vertical displacements. In this case, solutions are obtained to a normalizing coefficient, which can be determined from the available measurements or initial conditions.

Equation (7) and correspondingly its solution are very much similar to the solutions of the 1D Schrödinger equation for the probability of existence of a particle in the allowed energetic region. Solutions in this region have an oscillating wave character, and they decay beyond this region. The Schrödinger equation for the  $\psi$  function of probability is written as

$$\frac{d^2 \psi}{dz^2} + \frac{2m}{\hbar^2} [-V(z) + E] \psi = 0, \quad (9)$$

where  $E$  is the energy of the particle,  $V(z)$  is potential energy, and  $\hbar$  is Planck's constant.

The problem of possible generation of short internal waves in the shelf zone under consideration is similar to the problem of a particle in a potential well of finite depth. If the energy of the particle is  $E > V(z)$ , the solu-

tion is an oscillating function. In quantum mechanics, if energy is  $E < V(z)$ , this condition corresponds to a decay of the wave function in the classically forbidden region.

The two problems considered here are not fully similar because internal wave frequency  $\omega$  and energy  $E$  are differently included in similar equations. The similarity between solutions of these problems is in the fact that an internal wave can exist only in a thin pycnocline. The existence of the bottom is not necessary for the solution of the problem of internal waves in a sharp pycnocline layer. In the layer below the pycnocline, small values of the Brunt–Väisälä frequency do not allow the existence of an internal wave. Thus, the influence of large depth and the corresponding equations of long waves do not work here. The thickness of the pycnocline is the depth of the existence of internal waves. In this case, the wavelength is determined by the thickness of the layer of high vertical gradients of density. This thickness can be equal, for example, to 10 m or a few tens of meters. The length of such short waves, in principle, can be of the order of hundreds of meters, as was found in the spectral processing of satellite images.

## MATHEMATICAL MODELING OF SHORT INTERNAL WAVES

In this case, we solved a problem of local generation of the internal tide on the shelf of Oahu Island in the depth range up to 500 m due to the currents of the barotropic tide propagating to the bay and generating the internal tide over the slope of the shelf near the thermocline (pycnocline) layer. The maximal amplitudes of the internal tide in the ocean are generated when the barotropic tide currents flow over uneven topography. The appearing vertical components of the currents cause periodical displacements of isopycnal surfaces. The diurnal and semidiurnal tidal periods are energetic in the study region of Mamala Bay [2, 7, 12]. The tidal component corresponding to the M2 barotropic tide with a period of 12.4 h is the main energetic frequency of the internal tide.

The generation and propagation of tidal internal waves over the slopes of the bottom are investigated on the basis of numerical modeling using characteristic hydrological parameters for data input for the model. We used a 2D model of generation and propagation of internal waves in the shelf zone in coordinates directed normal to the coastline and along the depth [14]. Internal waves were considered plane waves propagating normal to the coast. The assumption about 2D properties of the developing wave processes practically does not change the characteristics of the internal wave field in the shelf and continental slope region, because the variability of internal waves in the direction normal to the coast is usually much stronger than the variability along the coastline.



The main source generating internal waves in the shelf region is the interaction between the currents of the barotropic tide and continental slope in the offshore part of the shelf [4, 15]. The currents of the barotropic tide and currents of semidiurnal internal waves generated over the deep parts of the Hawaiian Ridge incident at this slope in the shelf region obtain periodical vertical components, which cause the displacement of isopycnal surfaces, thus generating internal waves.

Water transport in the barotropic tide flow was specified on the basis of recalculation of the velocities of the barotropic tide to the stream function. The currents of the barotropic tide were estimated on the basis of data in [1, 2]. They were found from the condition of coincidence of the maxima of tidal currents of the diurnal and semidiurnal tides. For the model calculations, we used a work field 30 km long with a horizontal step of 10 m and 20 vertical levels. The time step was equal to 5 s. The coefficients of the horizontal eddy viscosity and density diffusivity were specified as  $11 \text{ m}^2/\text{s}$ , and the corresponding vertical coefficients were equal to  $0.0002 \text{ m}^2/\text{s}$ .

Internal waves generated over the slope of shelf depths for the M2 tide with a period of 12.4 h were calculated. The vertical density distribution was based on the data of measurements in the case of a sharp thermocline near the surface, which is formed at specific time moments [7, 9, 10, 12]. It was assumed that the sharp pycnocline layer was located at a depth of approximately 10–15 m. Analysis of the results of calculation by the described model is presented below.

## ANALYSIS OF RESEARCH RESULTS

Sections of the density field related to a specific phase of the M2 tide are obtained as a result of calculations. Figure 3 shows the calculated fields of specific densities. Sections of density fluctuations are presented for the time moment approximately corresponding to four M2 tidal periods from the beginning of calculations. The formation of an internal wave propagating over the shelf in the open ocean direction is clearly seen in Fig. 3. The density at the surface is specified as  $1.02256 \text{ kg/dm}^3$  (specific density is 22.56). Contour lines of density are shown with a step of  $0.00025 \text{ kg/dm}^3$ .

The results of modeling showed that a packet of short internal waves with an amplitude of ~10 m developing at a distance greater than 20 km off the coast is prominent in the section of specific density (Fig. 3). The length of waves in the packet is 150–200 m. This corresponds to a wave period of 4–5 min. The packet is generated when tidal perturbation propagates from the sharp slope of depths over a distance of approximately 15 km in the course of propagation of the perturbation

to the ocean. The faster frontal waves propagate ahead, while the short slower waves remain in the trailing part of the packet, which leads to its elongation. Such short internal waves can develop only in very narrow pycnocline located close to the surface. Such a wave does not exist in deeper layers and near the bottom.

If the amplitudes of short-period internal waves are equal to ~10 m, we can expect their manifestation at the surface. This was recorded in the spectra of satellite images in 2002–2004 (as was mentioned above, the lengths of such waves are equal to 80–200 m).

Thus, the investigations demonstrated that short internal waves are generated in a sharp pycnocline close to the surface. They are manifested at the surface and do not propagate deeper in the ocean. These short internal waves are revealed by means of spatial spectral processing of high-resolution (1 m) satellite images.

## REFERENCES

1. M. L. Eich, M. A. Merrifield, and M. H. Alford, *J. Geophys. Res.* **109** (C8), (2004). doi:10.1029/2003JC002049, 2004.
2. M. A. Merrifield and P. E. Holloway, *J. Geophys. Res.* **107** (C8), 3179 (2002).
3. V. G. Bondur, in *New Ideas in Oceanology* (Nauka, Moscow, 2004), Vol. 1, pp. 55–117 [in Russian].
4. V. G. Bondur, E. G. Morozov, G. I. Bel'chanskii, and Yu. V. Grebenyuk, *Issl. Zemli Kosmosa*, no. 2, 51 (2006).
5. *An Atlas of Internal Solitary-Like Waves and Their Properties*, Ed. by C. R. Jackson (Global Ocean Associates, Alexandria, 2004).
6. W. Krauss, *Internal Waves* (Gerbrüder Borntraeger, Berlin, 1966; Gidrometeoizdat, Leningrad, 1968).
7. V. G. Bondur, N. N. Filatov, Yu. V. Grebenyuk, Yu. S. Dolotov, R. E. Zdorovenkov, M. P. Petrov, and M. N. Tsidilina, *Oceanology* **47** (6), 3 (2007) [*Okeanologiya* **47** (6), (2007)].
8. B. A. Tareev, *Izv. Akad. Nauk, Fiz. Atmos. Okeana* **10**, 1064 (1966).
9. V. G. Bondur, in *Proc. of the 31 International Symposium on Remote Sensing of Environment* (St. Petersburg, 2005), pp. 215–217 [in Russian].
10. V. G. Bondur and N. N. Filatov, in *Proc. of the 7 Workshop on Physical Processes in Natural Waters, 2–5 July 2003* (Petrozavodsk, 2003), pp. 98–103 [in Russian].
11. V. G. Bondur, R. Keeler, and C. Gibson, *Geophys. Res. Lett.* **32**, L12610 (2005). doi:10.1029/2005GL022390.
12. V. G. Bondur, C. H. Gibson, R. N. Keeler, and P. T. Leung, *J. Appl. Fluid Mech.* **1**, 11 (2006).
13. V. G. Bondur and A. Sh. Zamshina, *Geodez. Aerofoto's'emka* **5**, 3 (2008).
14. V. I. Vlasenko, and K. Hutter, *J. Phys. Oceanogr.* **32**, 1779 (2002).
15. E. G. Morozov, *Deep Sea Research* **42**, 135 (1995).